Experimental study of multilayer gradient copper foam effect on pool boiling heat transfer performance and gas-liquid behavior characteristics

Chenggang Huang, Hui Wang, Eric Lichtfouse, Yikai Tang, Hengxue Xiang

▶ **To cite this version:**

Chenggang Huang, Hui Wang, Eric Lichtfouse, Yikai Tang, Hengxue Xiang. Experimental study of multilayer gradient copper foam effect on pool boiling heat transfer performance and gas-liquid behavior characteristics. International Journal of Thermal Sciences, 2023, 183, pp.107856. 10.1016/j.ijthermalsci.2022.107856 . hal-03752975

HAL Id: hal-03752975
https://hal.science/hal-03752975

Submitted on 17 Aug 2022

HAL is a multi-disciplinary open access archive for the deposit and dissemination of scientific research documents, whether they are published or not. The documents may come from teaching and research institutions in France or abroad, or from public or private research centers.

L'archive ouverte pluridisciplinaire **HAL**, est destinée au dépôt et à la diffusion de documents scientifiques de niveau recherche, publiés ou non, émanant des établissements d'enseignement et de recherche français ou étrangers, des laboratoires publics ou privés.

International Journal of Thermal Sciences 183 (2023) 107856

https://doi.org/10.1016/j.ijthermalsci.2022.107856

Experimental study of multilayer gradient copper foam effect on pool boiling heat transfer performance and gas-liquid behavior characteristics

Chenggang Huang [a], Hui Wang [a,*], Eric Lichtfouse [b], Yikai Tang [a], Hengxue Xiang [c]

[a] College of Environmental Science and Engineering, Donghua University, Shanghai, 201620, China
[b] Aix Marseille Univ, CNRS, IRD, INRAE, CEREGE, Aix-en-Provence, France
[c] State Key Laboratory for Modification of Chemical Fibers and Polymer Materials, Donghua University, Shanghai, 201620, China

ARTICLE INFO

Keywords:
Pool boiling
Heat transfer
Gradient copper foam
Gas-liquid behavior
Heat transfer mechanism

ABSTRACT

The rapid growth of the internet of things has induced the integration of many microelectronic devices in physical objects, yet the generated heat decreases the performance and stability of microelectronic devices. Therefore, new materials such as gradient metal foams (GMFs) have been recently designed to improve heat transfer. In this paper, an experimental visualization setup was built to investigate the effect of the GMFs gradient layers number and the arrangement order on the pool boiling heat transfer performance. Results show that increasing the number of gradient layers enhances the heat transfer when the copper foam pore density is low. By contrast, at high pore density of 50 PPI, increasing layers hardly changes heat transfer. The bubbles dynamic behavior on the metal foams surface of with different gradient structures is also different. When bubbles detach upward, the temperature of the metal foam is lower, and the temperature gradient is higher. When bubbles detach sideward, the bubble escape is much shorter, and the bubble detachment frequency and size increase. Combined with the theoretical research, the metal foam gas-liquid flow heat transfer model were constructed. The advantages and disadvantages of GMFs with different structures and the applicable scenarios are analyzed.

1. Introduction

The integration of electronic components in physical objects is rapidly increasing the era of the internet of things. Nonetheless, the performance and stability of microelectronic devices are reducing due to the generation of high temperatures locally. Therefore, heat transfer performance in electronic equipment should be improved [1]. Boiling heat transfer is an efficient mechanism for heat removal from a heated surface. Boiling heat transfer is classically improved by adjusting pressure and temperature [2], roughening the heating surface [3–5], increasing the heat transfer area [6], changing the surface wettability [7–11], and making a porous metal surface [11–14]. Recently, metal foams [15] have allowed better boiling heat transfer due to their high pore density, thermal conductivity and specific surface area. Metal forms absorb and diffuse fluids better, thus enhancing boiling heat transfer [16]. Copper foams of low pore density, about 10–30 PPI, show higher heat transfer than high pore density foams, above 50 PPI [17–20]. These studies show that heat transfer performance increases then decrease with pore density. The effect of metal foam thickness on the pool boiling heat transfer performance is similar to that of pore density, and the effect of different combinations of thickness and pore density varies greatly, and both parameters will instead inhibit the boiling heat transfer when they are too large [21,22].

The issue of the lower performance of boiling heat transfer at high pore density and thickness can be solved by using gradient metal foams, which are composites of two or more layers of metal foams with different pore densities. Indeed, GMFs enhanced heat transfer compared to the conventional open-celled uniform metal foam [23,24]. The gradient structure provided a reasonable path for escaping bubbles. An et al. came to the same conclusion and found that surface wettability significantly affects the GMFs [25]. Zhang et al. found that sodium dodecyl sulfate enhanced the pool boiling heat transfer of gradient foam at most heat flux, while n-heptanol deteriorated the pool boiling heat transfer [26]. Yang et al. observed that a radial gradient structure had better capillary performance than a uniform gradient structure [27]. Concerning layers arrangement, Xu et al. found that reversing a foam layer position highly influences the heat transfer [28–30]. The gradient structure bubble departure phenomenon was substantially attenuated as compared to the one-layer foam [31]. Huang et al. proposed three main ways for boiling bubbles to detach from the surface of gradient metal foams and found that adding self-wetting solutions significantly

* Corresponding author.
E-mail address: huiwang@dhu.edu.cn (H. Wang).

Nomenclature

cp	specific heat capacity ($J \cdot kg^{-1} \cdot K^{-1}$)
d	metal foam pore size (mm)
D	bubble size (mm)
f	bubble departure frequency (Hz)
h	surface coefficient of heat transfer ($W \cdot m^{-2} \cdot K^{-1}$)
H	thickness (m)
HGMFs	hybrid gradient metal foam (copper foam)
k	thermal conductivity ($W \cdot m^{-1} \cdot K^{-1}$)
n	layer numbers
$n\alpha$	active nucleation sites density
N_T	total number nucleation sites (#)
PGMFs	positive gradient metal foam(copper foam)
PPI	pores per inch (m^{-1})
q	heat flux ($W \cdot m^{-2}$)
S	total heat transfer area(m^2)
t	time (s)
ΔT	wall superheat (K)
x	distance from the thermocouple to block bottom (mm)

Greek symbols

ρ	density ($kg \cdot m^{-3}$)
α	thermal diffusivity ($m^2 \cdot s^{-1}$)
λ	thermal conductivity ($W \cdot m^{-1} \cdot K^{-1}$)
ω	pore density (PPI)
q	heat flux ($W^{-1} \cdot m^{-2}$)
ε	pore density (%)

Subscripts

w	wall
s	saturation
l	liquid
b	bubble
mf	metal foam

Table 1
Structure of seven composites of copper foam layers of various pore density and pore size and thickness. Layers are arranged from the top layer (left in table cells) toward the bottom layer (right in table cells).

Number	Pore density (PPI)	Pore size (mm)	Layer Thickness (mm)
1	20–40	1.27–0.0635	5–5
2	20-30-40	1.27-0.847-0.635	3.3-3.3-3.4
3	20-30-40-50	1.27-0.847-0.635-0.508	2.5-2.5-2.5-2.5
4	20-40-30-50	1.27-0.635-0.847-0.508	2.5-2.5-2.5-2.5
5	40-20-30-50	0.635-1.27-0.847-0.508	2.5-2.5-2.5-2.5
6	40-50-30-20	0.635-0.508-0.847-1.27	2.5-2.5-2.5-2.5
7	20-30-50-40	1.27-0.847-0.608-0.435	2.5-2.5-2.5-2.5

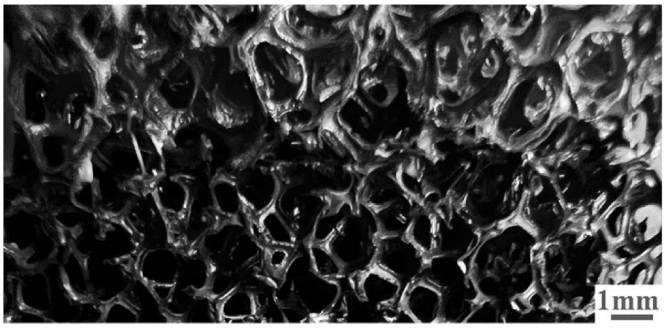

Fig. 1. 20–40 PPI Gradient copper foam composite made of an upper layer of 20 PPI metal foam and a lower layer of 40 PPI metal foam.

decreases heat transfer performance [32]. Wang et al. found that the boiling heat transfer performance of the metal foam cell with different gradient layer thicknesses was also different [33]. Mao et al. came to a similar conclusion [34]. Zhang et al. found that the GMFs can show superior pool boiling heat transfer performance in all heat flow density and pressure ranges [35].

Overall, GMFs show better heat transfer performance than single-layer metal foams. However, most studies on gradient structure have focused on two layers of metal foams, and there is few knowledge on multilayers. Little is also known on the movement of the external liquid and on the detachment of boiling bubbles, which control heat transfer. Therefore, here we studied the boiling heat transfer of copper foam in various gradient layers and structures using a visualization experimental setup. We investigated the behavior of boiling bubbles on the gradient copper foam surface. The gradient copper foam enhanced heat transfer mechanisms were investigated from the perspectives of the dynamic bubbles behavior and changes of macroscopic gas-liquid flow directions. The metal foams heat transfer models with different gas-liquid flow directions were constructed.

2. Experimental

2.1. Materials

We studied the boiling heat transfer of gradient metal foams, which are composites made of several layers of uniform copper foam of various pore density and thickness (Table 1, Fig. 1). Copper foams were purchased from Kunshan Guangjiayuanxin Material Company. GMFs with gradually increasing pore size from bottom to top are named positive gradient metal foams (PGMFs), e.g. 20-30-40-50 PPI, whereas other arrangements refer to hybrid gradient metal foams (HGMFs).

In this paper, in order to ignore the influence of other factors on the pool boiling heat transfer performance as much as possible, four kinds of copper foam with the same thickness of 20–30-40-50 PPI were selected and welded into different arrangements of gradient copper foam. From equation (8), we can see that the total heat transfer area of all GMFs was the same.

2.2. Analysis of the boiling heat transfer

Fig. 2 shows the system used to study the boiling heat transfer, including a heating system, a glass chamber, a data acquisition system, and a power supply system. The heating system comprises three 150 W dry-fired heating rods, auxiliary heaters, regulators, and power meters. The size of the glass chamber is 100×100 × 250 mm (L × W × H), and the outer wall of the chamber is composed of 4 pieces of 10 mm thick Plexiglas. The bottom plate is a Teflon plate with a small square hole of 21 mm side length in the center of the bottom plate for the heating copper block to pass through the bottom plate and contact the test medium (deionized water). The data acquisition system consists of a data acquisition instrument, a computer, K-type thermocouples, and a high-definition camera. The test is arranged with 6 thermocouples, where $T_1 \sim T_5$ are placed on the heating copper block with 6 mm spacing between two adjacent thermocouples, as shown in Fig. 3. T_6 is placed in the chamber to test the working medium's saturation temperature T_s.

It is necessary to used welding operations to ensure a tight connection between the metal foam and the heated copper block before the test starts. At this point, the thermal resistance of the solder layer is ignored

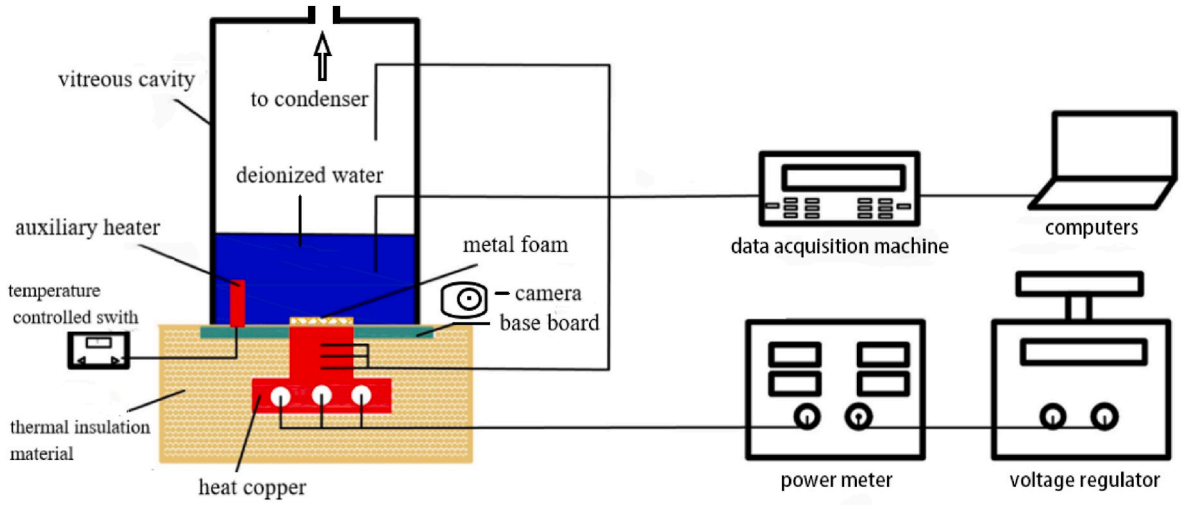

Fig. 2. Experimental system used to measure the boiling heat transfer.

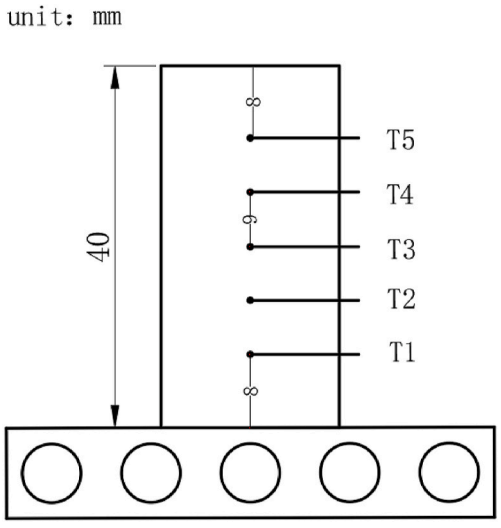

Fig. 3. Thermocouple arrangement on heated copper block (unit: mm).

in the data analysis because the thickness of the solder layer (<0.1 mm) is much lower than the thickness of the metal foam. The surface after soldering is shown in Fig. 4. The procedure is as follows: 1) the auxiliary heater is turned on to heat the test work medium to boiling for 20–30 min to ensure that the non-condensing gas dissolved in the test work medium is removed; then the auxiliary heater is turned off, allowing to cool for 2–3 h. 2) The auxiliary heater is turned on to heat and maintain the boiling state of the work medium in the cavity, then the heating rod is turned on at 10 W. 3) The temperature recorder is turned on. When the temperature fluctuation is lower than 0.1 K/30 min, we considered that the boiling pool has reached a stable state and we start to record the thermocouple temperature. 4) A camera takes pictures of the boiling work medium in the chamber. Then we increase the input power by + 5 W and repeat the previous steps. This is done until reaching 100 W. The heat flux of the pool boiling on the surface of copper foam is calculated according to the data derived from a computer. The change of heat flux with the increase of superheat can reflect the pool boiling heat transfer performance of copper foam, and the larger the heat flux, the stronger the pool boiling heat transfer performance.

Fig. 4. Metal foam soldered to a heated copper block.

2.3. *Data processing and uncertainty analysis*

A total of six thermocouples were arranged, of which T_1-T_5 were arranged on the heating copper block with two thermocouples spaced 6 mm apart. T_s recorded the temperature of the experimental work fluid, and since the thermal conductivity of the heating copper block is much larger than that of the insulation material, so the heating copper block can be approximated as a one-dimensional thermal conductivity only in the vertical direction.

The heat flux$q$ formula is derived from Fourier's law:

$$q = -\lambda \frac{dT}{dx}|_x \tag{1}$$

Since the copper block is approximately one-dimensional in thermal conductivity, the heating wall temperature can be obtained by linearly

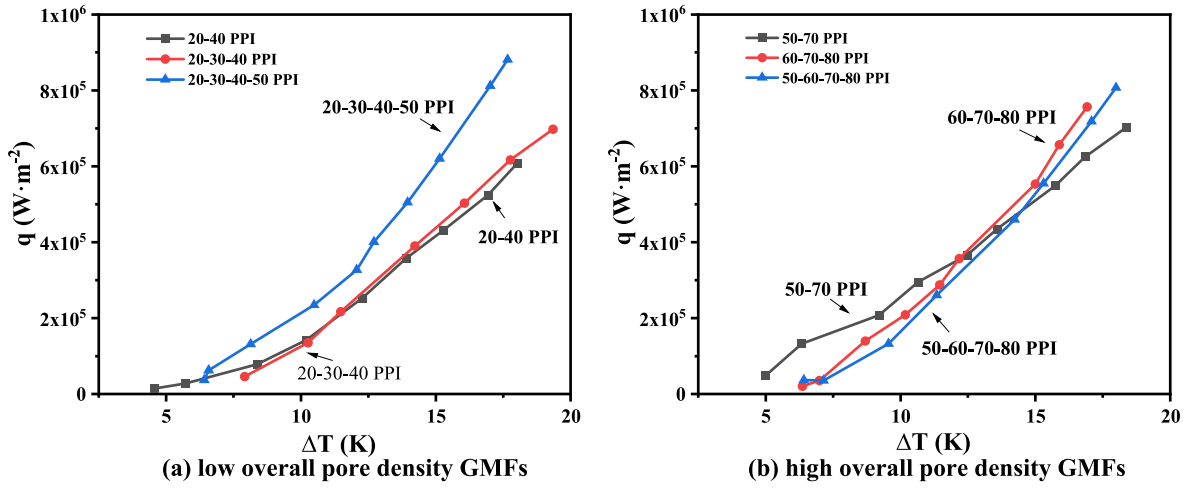

Fig. 5. Effect of the number of layers of gradient copper foam. Gradient Layers are arranged from the bottom layer toward the top layer, e.g. 20–40 refers to a two layer composite with a bottom layer of 40 PPI pore density and a top layer of 20 PPI pore density.

fitting T_1-T_5 measured by thermocouples to their corresponding x_1-x_5. $\lambda$is the thermal conductivity of the copper block, x_1-x_5 is the distance from the corresponding thermocouple measurement point to the bottom of the block.

Heating wall temperature T_w:

$$T_w = T = f(x_w, T) \tag{2}$$

where x_w is the height of the top surface of the thermally conductive copper column $x_w = 40$ mm.

Superheat degreeΔT calculation formula is as follows:

$$\Delta T = T_w - T_s \tag{3}$$

The convective heat transfer coefficient$h$ derived from the Newtonian cooling equation:

$$h = \frac{q}{\Delta T} = \frac{q}{T_w - T_s} \tag{4}$$

According to the UMF model [36], the total heat transfer area of the metal foam can be calculated from the following equation:

$$S_{total} \approx \sum_{i=1}^{n} V_i \sqrt{4(\pi + \pi^2)(1 - \varepsilon_i)} \Big/ d_{pi} \tag{5}$$

Where n is the number of layers of GMFs, Vandd_p are the volume of each layer of metal foam, metal foam pore size, respectively, which are calculated as follows:

$$V = 0.02 \times 0.02 \times H \tag{6}$$

$$d_p \approx 0.0254/\omega \tag{7}$$

Substituting equation (6) (7) into equation (5) yields the formula for calculating the total heat transfer area of the GMFs.

$$S_{total} \approx \sum_{i=1}^{n} 0.02 \times 0.02 \times H_i \times \omega_i \times \sqrt{4(\pi + \pi^2)(1 - \varepsilon_i)} \Big/ 0.0254 \tag{8}$$

In calculating the error of heat flux and heat transfer coefficient of the experimental system, the main sources of error according to the standard error analysis are thermocouple measurement error, thermocouple spacing error. According to the method of Moffat [37] the relative error equations for calculating the heat flux q and the surface heat transfer coefficient h can be obtained [38].

$$\frac{\Delta q}{q} = \sqrt{\left(\frac{\Delta T}{T}\right)^2 + \left(\frac{\Delta L}{L}\right)^2 + \left(\frac{\Delta \lambda}{\lambda}\right)^2} \le \frac{\Delta T}{T} + \frac{\Delta L}{L} + \frac{\Delta \lambda}{\lambda} \tag{9}$$

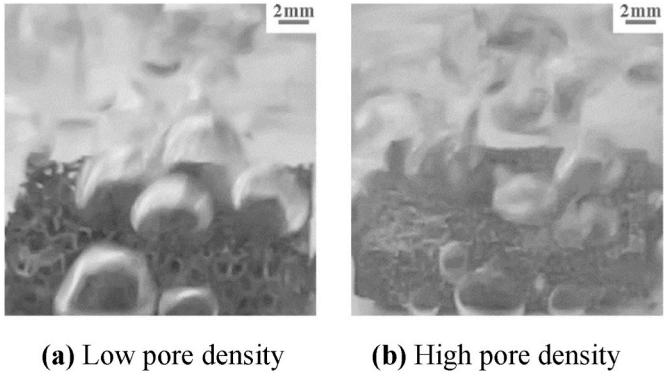

Fig. 6. Dynamic behavior of homogeneous open-cell metal foam bubbles. (a) Dynamic behavior of bubbles on the surface of low pore density metal foam (b) Dynamic behavior of bubbles on the surface of high pore density metal foam.

The calculated error of heat flux and heating surface temperature is less than 10%. The measurement error of thermocouple is 0.5%, and the error range is 1 K. The error of thermocouple measurement spacing is 3.3%, and the error of thermal conductivity of copper block is 3.1%. So, the maximum uncertainty of heat flux is 6.9%.

3. Results and discussion

3.1. Effect of the number of metal foam layers

Fig. 5 shows the boiling heat transfer performance on the gradient copper foam surface. The gradient copper foam is made of 2–4 layers of copper foam of same thickness (2.5 mm) and different pore densities, from 20 to 80 PPI. At low pore density, results show that the four-layer positive gradient 20-30-40-50 PPI, where 50 refers to the bottom layer just above the heat source, displays a higher heat transfer. This is likely due to easier bubble escape upward due to the increasing numbers of the layers. When the pore density is low, the heat transfer performance of pool boiling increases with the number of gradient copper foam layers. At high pore density, increasing the gradient layers number is no apparent effect. Indeed, the copper foam structure becomes more complex at high pore density, thus inducing a disordered movement of boiling bubbles (Fig. 6). Overall, we conclude that the positive multi-layer arrangement of copper foam displays a better heat transfer that the uniform layer.

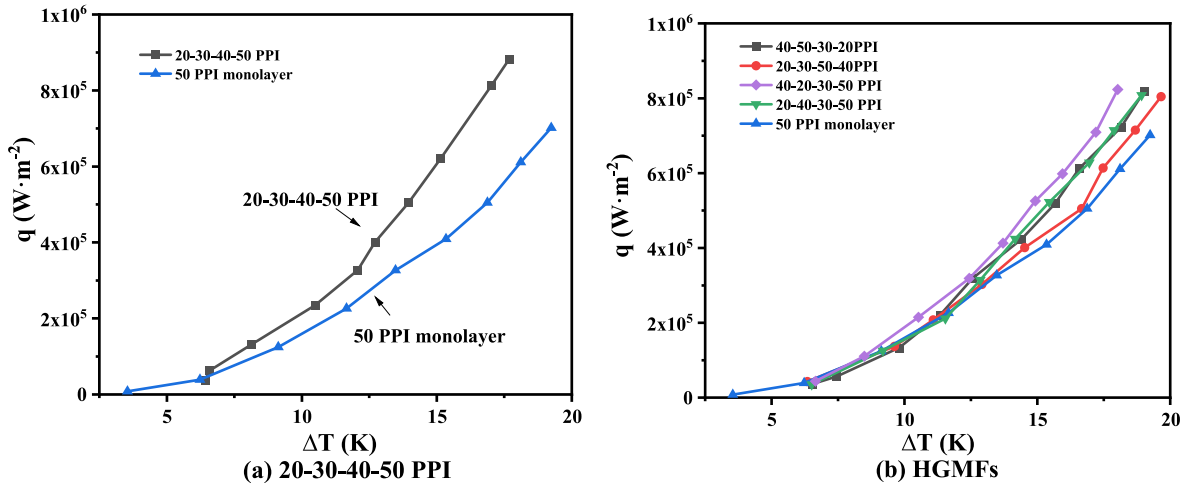

Fig. 7. Effect of different arrangements of gradient copper foam Layers are arranged from the bottom layer toward the top layer, e.g. 20-30-40-50 refers to a four layer composite with a bottom layer of 50 PPI pore density and a top layer of 20 PPI pore density. (a)positive gradient copper foam (b) hybrid gradient copper foam.

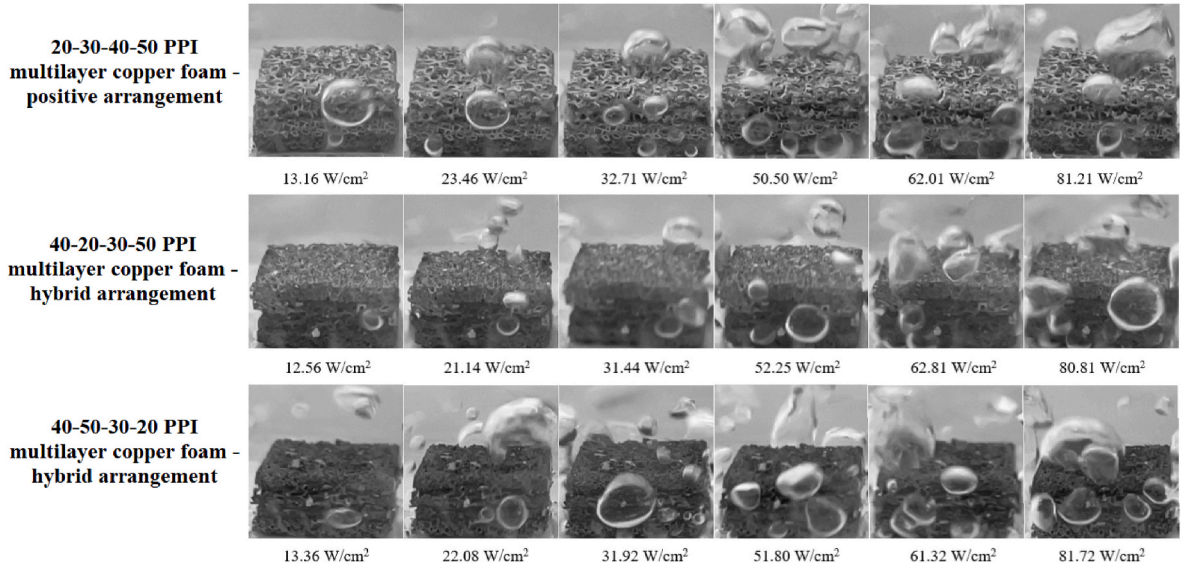

Fig. 8. Bubble dynamics versus heat flux in different arrangements of multilayers gradient copper foam. The 20-30-40-50 PPI multilayer, where 20 refers to the top layer just above the heat source, is a positive arrangement. The 40-20-30-50 PPI and 40-50-30-20 multilayers are hybrid arrangements.

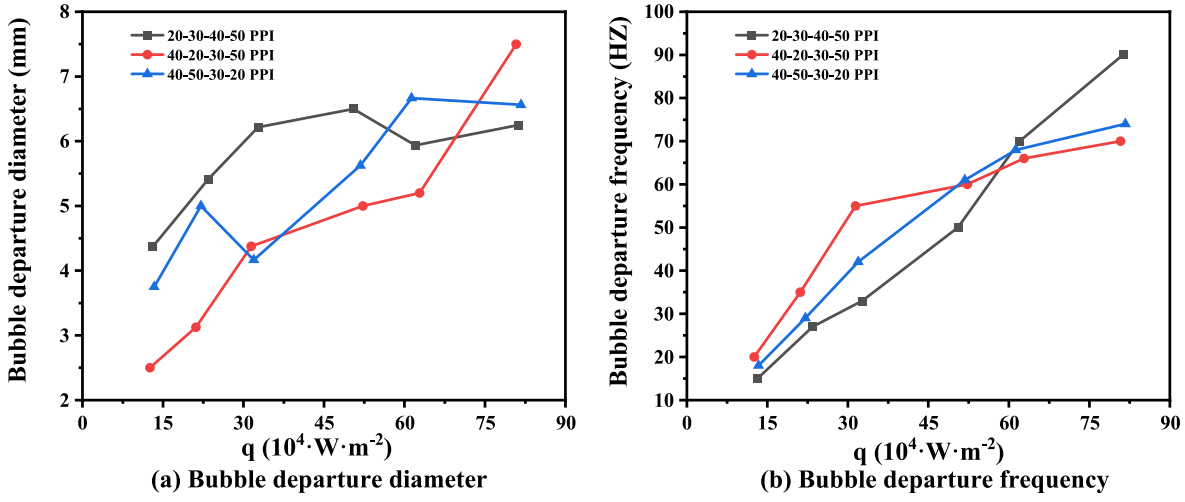

Fig. 9. Variation of the bubble departure frequency and bubble departure diameter with heat flux.

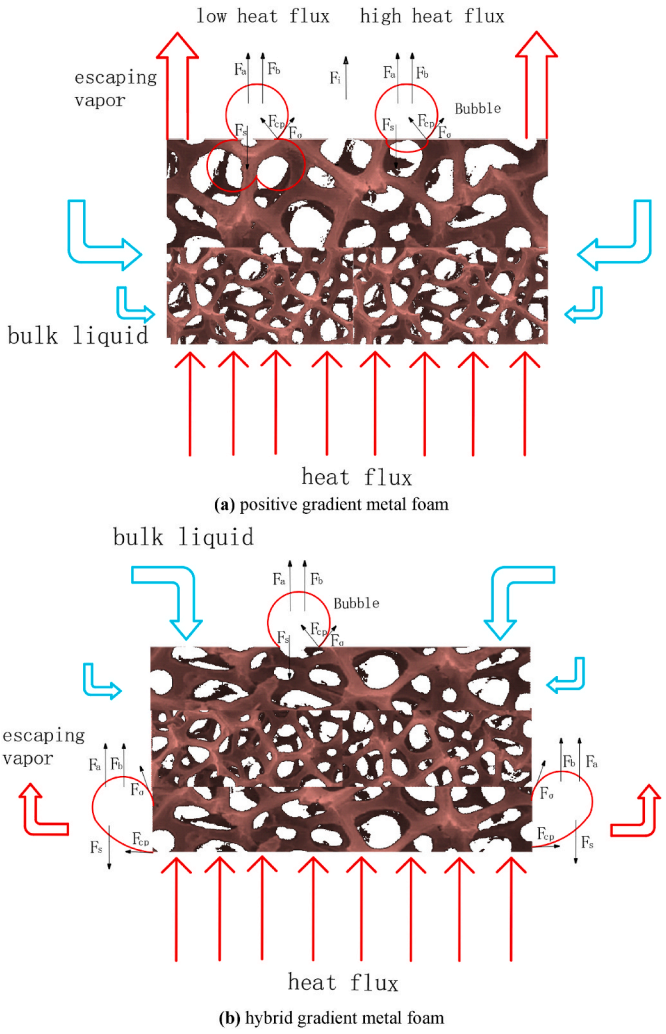

Fig. 10. Metal foam gas-liquid flow model and analysis of bubble detachment form (a)positive gradient metal foam (b)hybrid gradient metal foam. F_a is the bubble growth force, F_b is the heat flow driving force, F_i is the buoyancy force, F_{cp} is the contact pressure of the copper foam skeleton, F_S is the surface tension, and F_σ is the bubble brought by the metal foam skeleton escape resistance.

3.2. *Effect of layer arrangement on heat transfer*

Some studies showed that the gradient foam layer position change greatly influences the gas-liquid flow direction. We tested the effect of different arrangements of four copper foam layers of same thickness, of 2.5 mm, and different pore densities, from 20 to 50 PPI, on heat transfer (Fig. 7). Results show that all multilayer arrangements show higher boiling heat transfer performance than the 50 PPI uniform layer copper foam of 10 mm thickness. This is explained by gradient structure makes the pool boiling gas-liquid flow direction change, as detailed in the next section. We also observed that 20-30-40-50 PPI and 40-20-30-50 PPI layer arrangements had better heat transfer than other arrangements. The reasons will be further analyzed in the following text.

3.3. *Effect of layer arrangement on bubble dynamics*

The bubbles dynamics of multilayer gradient copper foam surface under different heat flux are displayed in Fig. 8. Bubble dynamics are very different. For instance, for the 20-30-40-50 PPI positive arrangement, where 50 refers to the bottom layer just above the heat source, bubble dynamic is very regular, most boiling bubbles come out of the copper foam surface from the top, and there is little interference and no merging of top bubble with lateral bubbles. By contrast, bubbles detach first from the sides for the 40-20-30-50 and 40-50-30-20 PPI hybrid layer arrangements. Then, in a second step, when nucleation sites of the upper copper foam are activated, some bubbles also detach from the top. Hybrid layer arrangements display more chaotic bubble detachment, more interference of bubbles with each other, closer positions of bubble detachment, and more bubble merging.

The bubble departure diameter could be directly estimated from the photograph taken in the boiling heat transfer by the camera. In this work, multiple photographs taken at the same stage were used to estimate the bubble departure diameter, and the averaged value was used. The bubble departure number is estimated from the high-speed videos, and then the departure frequency could be calculated from the bubble departure number. The separation size and frequency of bubbles under different heat flux were shown in Fig. 9. Results show that bubble size increases with heat flux. When boiling starts, the size of detached bubbles is higher on the 20-30-40-50 PPI positive layer arrangement than on hybrid layer arrangements. Then this difference reduces with boiling time. Larger bubbles at early stage are explained by a longer detachment path in the positive arrangement. As boiling progresses, the speed and number of bubble detachments rises, and bubble merging is more frequent in hybrid layer arrangements, leading to bigger bubbles at that

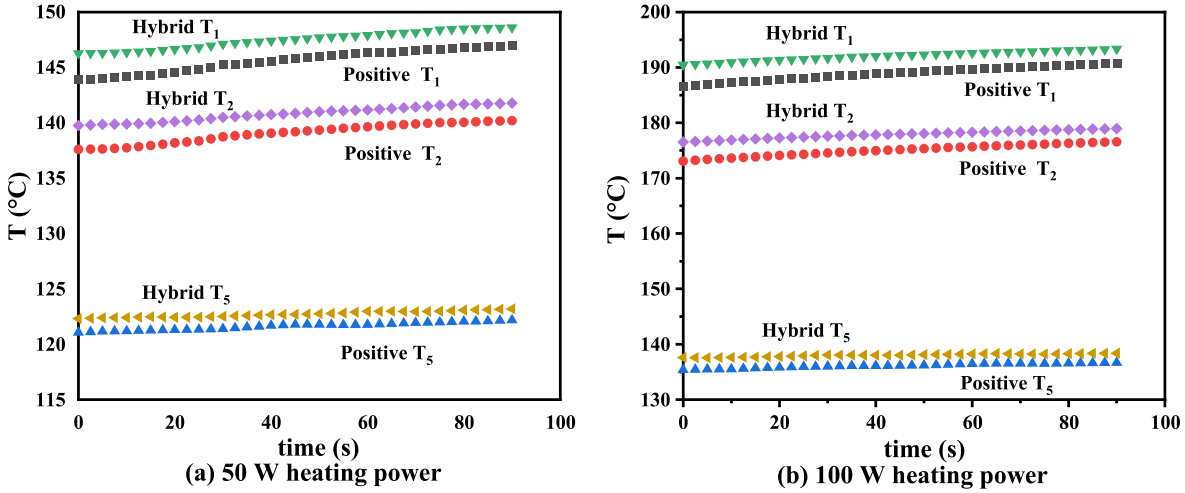

Fig. 11. Temperature at increasing height in positive and hybrid multilayers of copper foam. T_1 was taken at the bottom, and thus is the closest to the heat source. T_2 is located 6 mm above T_1, and so on. Positive refers to the 20 (bottom)-30-40-50 PPI layer arrangement. Hybrid refers to 20-40-30-50 PPI layer arrangement.

time and a disordered bubble dynamics behavior. Overall, for the positive layer arrangement, bubbles detach from the multilayer top and bubble size is more regular than for hybrid layer arrangements. For hybrid layer arrangements, bubbles detach initially from the sides and bubble size is irregular. For the bobble departure frequency, the bubble detachment frequency on the surface of HGMFs is higher than that on the surface of PGMFs at the early stage of boiling. As boiling continued, the frequency of bubble detachment on the surface of PGMFs increased more and more rapidly.

Based on experimental results, we drew gas-liquid flow models to explain the dynamics of the pool boiling bubbles (Fig. 10). For positive arrangements of multilayers of copper foam, e.g. 20-30-40-50 PPI, where 50 refers to the bottom layer just above the heat source, most bubbles detach from the top and the external liquid replenishes into the copper foam from the side. When the heat flux is low, the boiling bubble detach mainly from the surface by buoyancy. At this time, the boiling bubbles will interact inside the copper foam, and part of them will merge before escaping from the surface. Since bubbles merge first and then detach from the copper foam surface, the bubbles size detached in the low heat flux is not significantly smaller than those detached in the high heat flux, as shown in Fig. 9 (a) above. Then, when heat flux rises, bubble merging phenomenon decreases, most bubbles will be directly separated from the surface.

For hybrid arrangements of multilayers copper foam, e.g. 40-20-30-50 PPI, most boiling bubbles escape the copper foam surface from the side, at the initial stage, which greatly shortend the escape path. Thus, the HGMFs have a higher bubble detachment frequency at the beginning of boiling, as shown in Fig. 9 (b) above. At this time, the external liquid replenishes into the copper foam mainly from the top and upper side. Later, when bubbles start to detach from the top, the bubble disturbance becomes larger, and the external liquid replenishment position is reduced.

3.4. Heat transfer in multilayers of copper foam

In this paper, we studied heat transfer by thermocouple temperature T_1-T_5 in copper foams with different layer arrangement (Fig. 11). We compared the positive layer arrangement 20-30-40-50 PPI with the hybrid layer arrangement 20-40-30-50 PPI. Result show that the thermocouple temperatures of the positive gradient arrangement are always lower than that of the hybrid arrangements. This suggests that heat transfer mechanisms are different in positive and hybrid arrangements.

Literature reports show that transient heat conduction is the main heat transfer form in nucleation pool boiling [39,40]. The heat transfer process from the heating surface to the main liquid area can be regarded as a heat transfer from a hot surface to a semi-infinite object [41–43]. The total heat flow density of the transient thermal conductivity of the pool boiling heat transfer is given as:

$$q''_{\mathrm{tc}}(\mathrm{t}) = \frac{k_{\mathrm{l}}\Delta T}{\sqrt{\pi \alpha t}} \tag{10}$$

$$q''_{\mathrm{tc}} = \frac{2\pi k_{\mathrm{l}}(T_{\mathrm{w}} - T_{\mathrm{s}})}{A\sqrt{\pi \alpha_{\mathrm{l}}}} \sum_{n=1}^{N_{\mathrm{T}}} \left(D_{\mathrm{b,n}}^2 \left(\sqrt{t_{\mathrm{w,n}}} f_{\mathrm{b,n}} \right) \right) \tag{11}$$

From equation (11), it can be seen that the pool boiling transient thermal conductivity process is closely related to the bubble separation frequency (f) and the bubble separation diameter (D_b). Wang et al. [44] derived the pool boiling heat flux relationship based on the Rohsenow [45] correlation equation as:

$$Nu_{\mathrm{b}} = f(\mathrm{Re}_{\mathrm{b}}, Pr_{\mathrm{l}}) \tag{12}$$

$$q = 2(\pi k_{\mathrm{l}} \rho_{\mathrm{l}} c\mathrm{p}_{\mathrm{l}})^{1/2} f^{1/2} D_{\mathrm{b}}^2 n_{\alpha} (T_{\mathrm{w}} - T_{\mathrm{s}}) \tag{13}$$

In equation (13), $n\alpha$is the active nucleation sites density. As for the foam metal surface, due to its unique porous structure, the pool boiling transient thermal conductivity process will take place inside the pores. So, we use the pores number of metal foam pores number Nmf instead of the active nucleation sites density $n\alpha$. Based on equation (13), we can derive the correlation equation for boiling heat transfer on GMFs surface as:

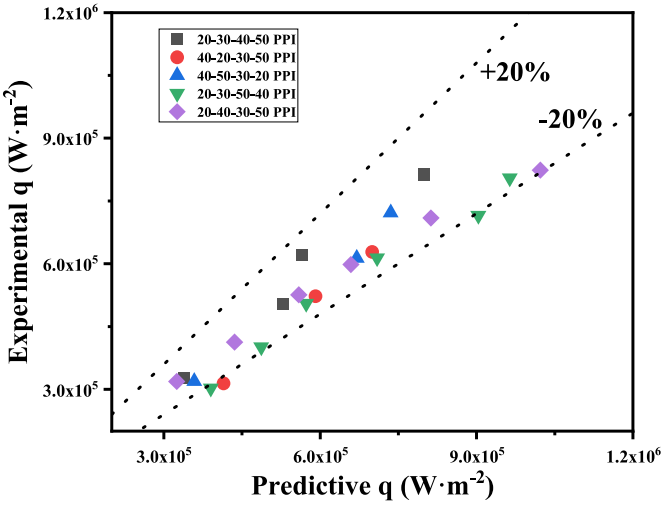

Fig. 12. Prediction accuracy of correlation for gradient metal foams.

$$q_{\mathrm{mf}} = 2EF_{\mathrm{mf}}\eta N_{mf}(\pi k_{\mathrm{l}}\rho_{\mathrm{l}}c\mathrm{p}_{\mathrm{l}})^{1/2} f^{1/2} D_{\mathrm{b}}^2 (T_{\mathrm{w}} - T_{\mathrm{s}}) \tag{14}$$

$$EF_{\mathrm{mf}} = \frac{S_{\mathrm{mf}}}{S_{base}} \tag{15}$$

Due to the foam metal stereoscopic structure, it can significantly increase the boiling heat transfer area. So, EFmf is defined as the correction factor for boiling heat transfer in the foam metal surface. For the pore number Nmf, there is a calculation error. Meanwhile, equation (13) is a theoretical formula, so we need to introduce a correction factor η to correct Nmf. This is due to the complex structure of the foam metal, the bubble clogging phenomenon or the untimely rewetting process will lead to most of the foam metal area cannot carry out the complete pool boiling process. Where the correction factor η is 0.0965 for the PGMFs and 0.101 for the HGMFs.

The prediction accuracy of the new correlation is shown in Fig. 12. The predicted values of the correlation can agree with 95% of the experimental data within a deviation of ±20%.

From equation (14), it can be seen that the GMFs pool boiling heat transfer performance is positively correlated with the bubble separation frequency (f) and the bubble separation diameter (D_b). Shortening the bubble escape distance can thus enhance the transient heat conduction process of pool boiling and enhance the pool boiling heat transfer performance.

It is assumed that when the bubble breaks away from the wall, the bubble takes away the liquid in an area whose radius is the size of the bubble's breakaway diameter. At the same time the cold liquid rushes to the heated surface, generating strong transient heat conduction. In the metal foam, when the bubble breaks away from the copper foam surface along the path, the external liquid immediately replenishes to the inside of the metal foam for rewetting, thus inducing transient heat conduction. Moreover, due to the porous nature of the metal foam itself, the number of pores is large, and the transient heat conduction will be carried out in each pore. This fully reflects the advantage of bubble nucleation points number of metal foam.

When the bubble is detached upward, the boiling bubble keeps contact with the metal foam skeleton in the detachment process, thus taking away the heat of the copper foam skeleton. The heat of the metal foam skeleton increases the bubble diameter and enhances the transient thermal conductivity (Fig. 13). This finding is consistent with models

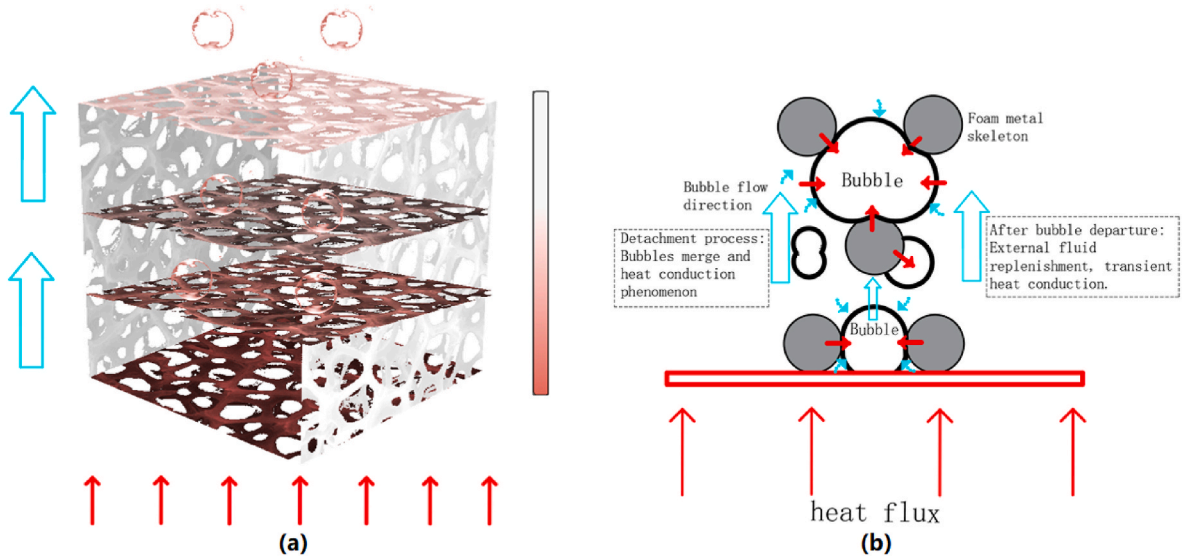

Fig. 13. Bubble top detachment heat transfer model (a) Macroscopic heat transfer (b) bubble escape path.

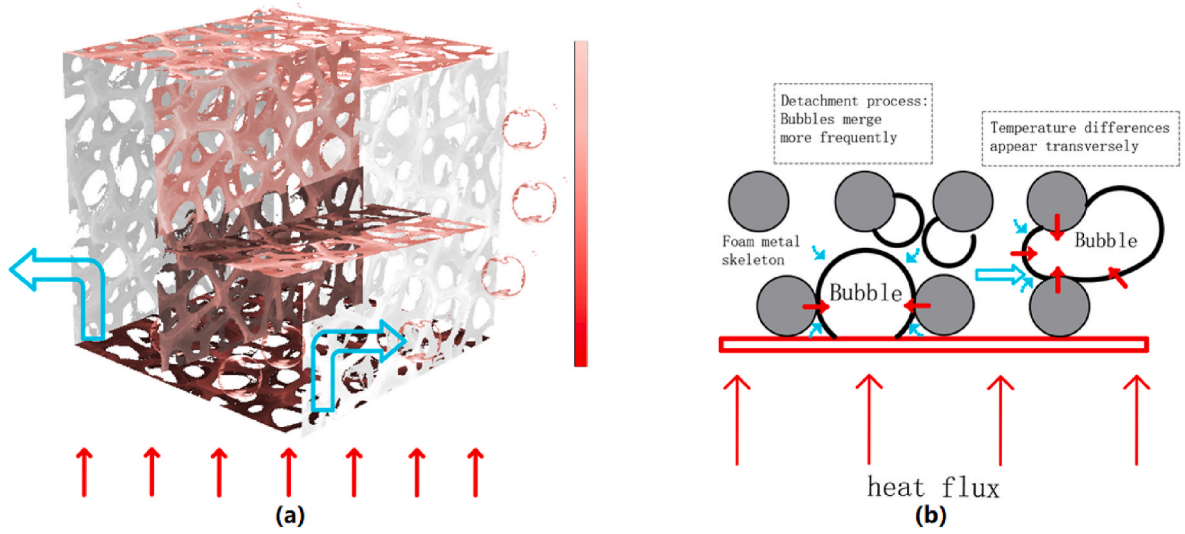

Fig. 14. Bubble side detachment heat transfer model (a) Macroscopic heat transfer (b) bubble escape path.

such as Dhir and Liaw's [46] and Zhao et al.'s [47]. Furthermore, the process of bubble detachment is often accompanied by bubble merging, which promotes the rewetting process of pool boiling. The transfer of heat from the metal foam skeleton causes the overall temperature of the metal foam to drop, promoting the boiling heat transfer. Thus, for the PGMFs, the boiling heat transfer performance is mainly determined by the number of bubble nucleation points.

When the detachment direction of the bubble changes from the top to the side, the upper metal foam and the boiling bubble do not carry out heat transfer. This leads to a decrease in the temperature gradient of the longitudinal metal foam and a temperature difference in the lateral direction, with the internal temperature of the metal foam being closer, as shown in Fig. 14. From the heat transfer point of view, the lateral detachment is not conducive to the boiling heat transfer. However, when the bubble breaks away from the metal foam side, the escape path of the bubble becomes shorter, the merging phenomenon of bubbles occurs frequently, and the escape speed and frequency of the bubble are higher. The rapid detachment of bubbles promotes the rewetting process of pool boiling, strengthening the transient heat conduction process, and facilitating heat transfer. Thus, for the HGMFs, the dynamic behavior of bubbles is the decisive factor affecting the boiling heat transfer performance. This explains why heat transfer enhancement is similar for positive and hybrid arrangements (Fig. 7), despite different temperature readings (Fig. 11). For the positive layer arrangement, temperature readings are lower due to the upward movement of the bubble, which results in a larger overall temperature gradient in the copper foam.

According to the experimental results above, we found that PGMFs and HGMFs have different enhanced boiling heat transfer mechanisms, and thus have different advantages and disadvantages. Combined with the previous study, it can be found that the PGMFs can effectively reduce the heating surface temperature, which is very suitable for those engineering scenarios where the heating surface temperature needs to be controlled. The HGMFs enhance the boiling heat transfer performance by changing the direction of gas-liquid flow in the pool boiling. Compared with the PGMFs, The heat transfer properties of HGMFs require very low physical parameters of the metal foam, which can be used to save materials in some specific applications.

4. Conclusion

In this paper, the boiling heat transfer characteristics of multilayer GMFs were experimentally studied. The strengthening mechanism of different GMFs was investigated in detail, and the following conclusions were drawn:

(1) For low pore density copper foam, the boiling heat transfer performance increases with the increase of the foam layers. However, for high pore density copper foam, the boiling heat transfer performance hardly changes with the number of the foam layers.
(2) The dynamic behavior of bubbles on the PGMFs surface is regular and orderly. In contrast, the behavior of bubbles on the HGMFs surface is disorderly and chaotic. The gas-liquid flow model of metal foam is obtained by analyzing the bubbles dynamic behavior of different structure metal foam.
(3) Both gradient structure metal foams can enhance the transient thermal conductivity of the pool boiling process. The PGMFs surface detached bubbles can take away more heat from the metal foam skeleton, and the temperature gradient is large. The escape path of HGMFs bubbles is greatly reduced, and the size and frequency of escape bubbles increase.
(4) The superiority of the boiling heat transfer performance of the two gradient structures was demonstrated experimentally. Among them, the PGMFs can better reduce the heating surface temperature, while the HGMFs have lower requirements for metal foam parameters.

Declaration of competing interest

The authors declare that they have no known competing financial interests or personal relationships that could have appeared to influence the work reported in this paper.

Data availability

The data that has been used is confidential.

Acknowledgments

The study was funded by State Key Laboratory for Modification of Chemical Fibers and Polymer Materials, Donghua University (KF2123) and Shanghai Sailing Program (19YF14011700).

References

[1] W. Cao, Experimental Study on the Enhancement of Flow and Boiling Heat Transfer in Copper Foam [D], Jiangsu University of Science and Technology, 2020.
[2] X.G. Fan, L. Yang, M. Zhang, Saturated pool boiling with HFE-7100 on a smooth copper surface under different pressures [J], Chem. Ind. Eng. Prog. 40 (1) (2021) 57–66.
[3] S. Armin, T. Outi, C. Mauro, et al., Effects of surface nanostructure and wettability on pool boiling: a molecular dynamics study[J], Int. J. Therm. Sci. 167 (2021), 106980.
[4] K. Robert, P. Robert, Pool boiling of water on surfaces with open microchannels[J], Energies 14 (11) (2021) 3062, 3062.
[5] H.M. Kurihara, J.E. Myers, The effects of superheat and surface roughness on boiling coefficients[J], AIChE J. 6 (1) (1960) 83–91.
[6] H. Zhang, X.L. Wang, Y. Du, et al., Influence of heating surface size on heat transfer performance of saturated pool boiling [J], J. Xi'an Univ. Sci. Technol. 41 (3) (2021) 417–424.
[7] J. Zhou, P.Z. Xu, B.J. Qi, et al., Effects of micro-pin-fins on the bubble growth and movement of nucleate pool boiling on vertical surfaces[J], Int. J. Therm. Sci. 171 (2022), 107186.
[8] W.J. He, Study on Boiling Condensation Characteristics of Superhydrophilic Hydrophobic Composite Surface Based on LBM Method [D], Inner Mongolia University of Science and Technology, 2020.
[9] M.S.K. Moha, L. Ference, Enhancement of pool boiling heat transfer performance using dilute cerium oxide/water nanofluid: an experimental investigation[J], Int. Commun. Heat Mass Tran. 114 (2020), 104587.
[10] Y. Zhu, H.T. Hu, G.L. Ding, et al., Influence of oil on nucleate pool boiling heat transfer of refrigerant on metal foam covers[J], Int. J. Refrig. 34 (2) (2010) 509–517.
[11] K. Hyungdae, K.D. Eok, Effects of surface wettability on pool boiling process: dynamic and thermal behaviors of dry spots and relevant critical heat flux triggering mechanism[J], Int. J. Heat Mass Tran. 180 (2021), 121762.
[12] Y. An, C.L. Huang, X.D. Wang, Effects of thermal conductivity and wettability of porous materials on the boiling heat transfer[J], Int. J. Therm. Sci. 170 (2021), 107110.
[13] D.C. Mo, S. Yang, J.L. Luo, et al., Enhanced pool boiling performance of a porous honeycomb copper surface with radial diameter gradient[J], Int. J. Heat Mass Tran. 157 (2020), 119867.
[14] A.S. Katarkar, A.D. Pingale, S.U. Belgamwar, et al., Experimental study of pool boiling enhancement using a two-step electrodeposited Cu-GNPs nanocomposite porous surface with R-134a[J], J. Heat Tran. (2021), 121601.
[15] H. Wang, L.J. Guo, K. chen, Theoretical and experimental advances on heat transfer and flow characteristics of metal foams[J], Sci. China Technol. Sci. 63 (5) (2020) 705–718.
[16] L.L. Manetti, G. Ribatski, R. Souza, et al., Pool boiling heat transfer of HFE-7100 on metal foams[J], Exp. Therm. Fluid Sci. 113 (2020), 110025.
[17] S. Moghaddam, M. Ohadi, J. Qi, Pool Boiling of Water and FC-72 on Copper and Graphite Foams[C], Asme International Electronic Packaging Technical Conference & Exhibition, 2003, pp. 675–680.
[18] J.L. Xu, X.B. Ji, W. Zhang, et al., Pool boiling heat transfer of ultra-light copper foam with open cells[J], Int. J. Multiphas. Flux 34 (11) (2008) 1008–1022.
[19] X. Jia, Study on Pool Boiling Heat Transfer Enhancement with Copper Foams [D], Southeast University, 2018.
[20] R. Liu, Z.C. Teng, S.G. Yao, et al., Effects of different concentrations of Al2O3 nanoparticles and base fluid types on pool boiling heat transfer in copper foam with bottom condensed reflux[J], Int. J. Therm. Sci. 163 (2021), 106833.
[21] L.L. Manetti, A. Moita, R. Souza, et al., Effect of copper foam thickness on pool boiling heat transfer of HFE-7100[J], Int. J. Heat Mass Tran. 152 (2020) 119547.1–119547.15.
[22] M. Calati, G. Righetti, L. Doretti, et al., Water pool boiling in metal foams: from experimental results to a generalized model based on artificial neural network[J], Int. J. Heat Mass Tran. 176 (1599) (2021), 121451.
[23] Z.G. Xu, C.Y. Zhao, Y. Zhao, Experimental investigation on pool boiling heat transfer of gradient metal foams[J], J. Eng. Thermophys. 36 (10) (2015) 2240–2244.
[24] S. Mou, Investigation on Pool Boiling Heat Transfer of Gradient structures[D], Shanghai Jiao Tong University, 2019.
[25] An Y , Huang C L , Wang X D . Effects of thermal conductivity and wettability of porous materials on the boiling heat transfer[J]. Int. J. Therm. Sci., 170.
[26] Z.H. Zhang, S. Mou, Z.G. Xu, et al., Experimental investigation on pool boiling mechanism of the gradient metal foam[J], Int. Heat Tran. Conf. 16 (2018).
[27] S. Yang, Preparation and Pool Boiling Performance of Gradient Porous Copper Structure [D], Sun Yat-sen University, 2020.
[28] Z.G. Xu, S. Mou, Q. Wang, et al., Experimental investigation on pool boiling mechanism of two-level gradient metal foams in deionized water, aqueous surfactant solutions and polymeric additive solutions[J], Exp. Therm. Fluid Sci. 96 (2018) 20–32.
[29] Z.G. Xu, M.Q. Wang, C.Y. Zhao, Investigation on pool boiling heat transfer of metal foam with gradient pore densities[J], J. Therm. Sci. Technol. 14 (2) (2015) 106–113.
[30] Z.G. Xu, J. Qin, Pool boiling investigation on gradient metal foams with double layers[J], Appl. Therm. Eng. 131 (2018) 595–606.
[31] L.P. Zhou, W. Li, T.X. Ma, et al., Experimental study on boiling heat transfer of a self-rewetting fluid on copper foams with pore-density gradient structures[J], Int. J. Heat Mass Tran. 124 (2018) 210–219.
[32] R.L. Huang, C.Y. Zhao, Z.G. Xu, Investigation of bubble behavior in gradient porous media under pool boiling conditions[J], Int. J. Multiphas. Flux 103 (2018) 85–93.
[33] Y.K. Wang, Experimental Study on Pool Boiling Heat Transfer Characteristics of Surface Modified Porous Copper [D], China University of Mining and Technolog, 2021.
[34] Y.B. Mao, W. Chen, J. Wang, The heat transfer characteristics of open-cell metal foams in pool boiling [J], Cryog. Supercond. 43 (6) (2015) 79–83.
[35] S.L. Zhang, Experimental Study on Boiling Heat Transfer of Different Structural Parameter Copper Foams under Different Pressures [D], Jiangsu University of Science and Technology, 2017.
[36] Y.P. Du, C.Y. Zhao, Y. Tian, et al., Analytical considerations of flux boiling heat transfer in metal-foam filled tubes[J], Heat Mass Tran. 48 (1) (2012) 165–173.
[37] R.J. Moffat, Describing the uncertainties in experimental results[J], Exp. Therm. Fluid Sci. 1 (1) (1988) 3–17.
[38] S. Sarangi, J.A. Weibel, S.V. Garimella, Effect of particle size on surface-coating enhancement of pool boiling heat transfer[J], Int. J. Heat Mass Tran. 81 (2015) 103–113.
[39] J.L. Bi, X.P. Lin, D.M. Christopher, Effects of bubble coalescence dynamics on heat flux distributions under bubbles[J], AIChE J. 59 (2013) 1735–1745.
[40] S. Moghaddam, K. Kiger, Physical mechanisms of heat transfer during single bubble nucleate boiling of FC-72 under saturation conditions. II: theoretical analysis[J], Int. J. Heat Mass Tran. 52 (5–6) (2009) 1295–1303.
[41] J.L. Bi, Y.P. Huang, J.J. Xu, et al., Study of nanofluid saturated pool boiling heat transfer and CHF model [J], Atomic Energy Sci. Technol. 51 (6) (2017) 1008–1015.
[42] Y. Han, P. Griffith, The mechanism of heat transfer in nucleate pool boiling-Part I [J], Int. J. Heat Mass Tran. 8 (6) (1965) 887–904.

[43] C. Cerardi, J. Buongiorno, L.W. Hu, et al., Study of bubble growth in water pool boiling through synchronized, infrared thermometry and high-speed video[J], Int. J. Heat Mass Tran. 53 (19) (2010) 4185–4192.
[44] B.X. Wang, C.H. Li, D.S. Wen, et al., A revision on Rohsenow model for nucleate boiling of liquid with considering the effect of surface wettability[J], J. Eng. Thermophys. (1) (2002) 79–81.
[45] W.M. Rohsenow, A method of correlating heat transfer data for surface boiling of liquids[J], Trans. ASME 74 (1952) 969–976.
[46] V.K. Dhir, S.P. Liaw, Framework for a unified model for nucleate and transition pool boiling[J], J. Heat Tran. 111 (3) (1989) 739.
[47] Y.H. Zhao, T. Masuoka, T. Tsuruta, Unified theoretical prediction of fully developed nucleate boiling and critical heat flux based on a dynamic microlayer model[J], Int. J. Heat Mass Tran. 45 (15) (2002) 3189–3197.